Generation and Characterization of Fork Gratings in Fused Silica

Sebastian Buettner, Erik Thieme and Steffen Weissmantel
Laserinstitute Hochschule Mittweida, Technikumplatz 17, Mittweida, Germany

Keywords: Fork Grating, Orbital Angular Momentum, Fluorine Laser, Fused Silica, Calcium Fluorine Mask, Micro Structuring, Micro Machining, Direct Laser Fabrication.

Abstract: Fluorine laser micro structuring enables the generation of fork gratings in fused silica. These micro-optical elements can be used to influence the orbital angular momentum of light. This property of light has been researched for more than 30 years and is becoming increasingly interesting for various applications. One of them is optical data communication, where this can be used to increase the transmission capacity of optical fibers. Now we have been able to demonstrate a simple fabrication method based on the fluorine laser micro structuring technique, which allows us to generate different types of gratings. The results of our investigations as well as those of the geometrical and optical characterization are presented.

1 INTRODUCTION

Electromagnetic (EM) fields are well understood since Maxwell. The wavelength, polarization, amplitude and phase are the common properties to describe these fields. Each of mentioned can be influenced and modulated by optical elements or devices according to the requirements of the technical application. In particular, the optical data communication is based on the (de-)modulation of these properties. This allows a simultaneous transmission of optical signals. In the field of optical data communication different, so called, multiplexing methods were developed to increase the data rate. The multiplexing methods, which, based on the wavelength or polarization, cannot be developed further due to the limited capacity of optical channels. These limitations are caused by nonlinear effects, due to the high intensities within the fibers (Richardson, 2010). One solution for this problem could be using the orbital angular momentum (OAM) of EM fields for multiplexing purposes (Xie et al., 2018 and Bozinivic et al., 2013). However, the OAM is an interesting property which also can be used for other technical applications like optical tweezers. This allows the rotation of microscopic particles by laser light (Yao et al., 2011). Moreover, quantum optical methods allow the entanglement of OAM states of photons. This enables the development of new techniques in the field of quantum optics (Mair et al., 2001, Fickler et al. 2012 and Fickler et al., 2018). In the last years several methods for micro-optics fabrication were developed too, which allows the miniaturisation and integration of micro-optics. First and foremost, photolithography is a process for creating highly precise microstructures. But the process is expensive and time-consuming. Our investigations show that we can fabricate irregular micro-structures such as fork gratings in a much easier way. For this we developed a fluorine laser micro structuring method, which allows us to generate individual grating geometries within a few milliseconds. Moreover, we could show that these gratings already can be used for OAM manipulation. Accordingly, our process is verry suitable for an efficient and flexible integration of these kinds of optical elements and potentially for the development of new communication hardware.

2 FUNDAMENTALS

In 1992 Les Allen and colleagues (Allen et al., 1992) could show that electromagnetic fields include angular momentum.

$$\vec{J} = \epsilon_0 \int \vec{r} \times (\vec{E} \times \vec{B}) dr \quad (1)$$

Moreover, it is shown that the total angular momentum is composed by the spin angular momentum $\vec{s}$ and the orbital angular momentum $\vec{l}$. The spin angular momentum (SAM) is associated

Buettner, S., Thieme, E. and Weissmantel, S.
Generation and Characterization of Fork Gratings in Fused Silica.
DOI: 10.5220/0011685500003408
In *Proceedings of the 11th International Conference on Photonics, Optics and Laser Technology (PHOTOPTICS 2023)*, pages 40-45
ISBN: 978-989-758-632-3; ISSN: 2184-4364

with a circular polarization, whereas the orbital angular momentum is resulting from a spatial distribution.

$$\vec{J} = \underbrace{\frac{\epsilon_0}{2i\omega}\int \sum_{j=x,y,z} E_j^*(\vec{r}\times\nabla)\,E_j\,d^2r}_{\vec{l}} + \underbrace{\frac{\epsilon_0}{2i\omega}\int E^*\times E\,d^2r}_{\vec{s}} \quad (2)$$

More precisely, the orbital angular momentum results from a helical phase shift, which, for example, can be observed in Gaussian-Laguerre laser modes. However, such a phase can also be induced by a phase element that modulates an even EM field with an amplitude $u_0(r,\varphi,z)$.

$$u(r,\varphi,z) = u_0(r,z)\cdot e^{-ikz}\cdot e^{il\varphi} \quad (3)$$

The expression $e^{il\varphi}$ describes an azimuthal dependency of the phase, where φ is the azimuthal angel and l the topological charge (TC) (Allen et al. 2009 and 2011). There are several methods to induce or influence the OAM of an EM field. As mentioned, the Gaussian-Laguerre laser modes have an intrinsic OAM which can be changed e.g., by a cylindrical lens. Furthermore, it is possible to convert SAM to OAM by anisotropic materials (Marrucci et al., 2006) and q-plates (Karimi et al., 2009).

Back to the phase modulation, OAM can be induced by optical elements like spiral phase plates (SPP) or fork gratings (FG). These elements changing the phase of an EM wave with an azimuthal dependency. The phase shift results from an azimuthal change of the optical thickness within a transparent material. Due to the fabrication process SPPs resemble a spiral staircase and can be generated by changing the optical thickness of a substrate step by step. In the case of SPPs, the TC defines the number of 2π phase jumps within the structure, which also represents the gear number of a helical modulated wave front. The sign of l gives the sense of rotation of the phase, which is also called handedness. Depending on the transition direction of the optical elements, the handedness of the modulated EM field is ether the same or inverted to the one of the structures. Other than SPPs, FGs are a superimposition of a helical phase and a grating phase. Therefore, the helical phase is hidden within the grating structure and can be recognized by the ending grating bars and grooves within the structure. The higher the TC, the more grating bars and grooves ending within the structure.

FGs work slightly different relating to the OAM modulation. In general, optical gratings bend the light in one or more diffraction orders. Therefore, FGs modulate and bend the light simultaneous and in a different way for each diffraction order. The higher the diffraction order, the higher is the OAM of these order. Diffraction orders with an opposite sign also show a different handedness, which is a result of the law of conservation of momentum. For the generation and examination of FGs, in addition to understanding the function of the optical elements, their calculation is necessary. The calculation of those gratings was done using the numerical calculation software Matlab®. Moreover, we basically follow the solution of Galvez (Galvez E., 2016) to calculate the FG layouts. The source code for calculation is given in Table 1. In Figure 1 a) the calculated continuous phase distribution of an FG with a TC of 1 is shown. The developed fabrication process requires the generation of a projection masks. For this, the phase distribution must be converted into a binary, which is done by a rounding operation (see Figure 1 b)). From this, we can extract the grating geometry for the mask generation.

Table 1: MATLAB®-Source for calculation of FGs.

```
N=500; l=1; n=10;
x=linspace(-N/2,N/2,N);
[X,Y]=meshgrid(x,x);
[phi,R]=cart2pol(X,Y);
bl=linspace(0,n*2*pi,N).*ones(N,N)
phase=round(mod(phi*l+bl,2*pi)/(2*pi));
```

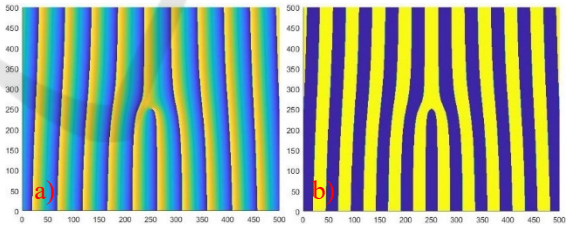

Figure 1: Calculated phase distribution of a blazed fork grating a) and its binary representation b).

Moreover, the knowledge of the micro structuring depth is necessary for the FG generation. For a 2π phase shift, the depth depends on the design wavelength λ and the refractive indices of the substrate n_1 and the continuum n_0. It can be calculated using equation 4.

$$h = \frac{\lambda}{n_1 - n_0} \quad (4)$$

For our investigations we used the fused silica corning 7980. The refractive index of the material

($n_1 = 1.4607$) was calculated by the Sellmeier equation for a wavelength of $\lambda = 532\ nm$. This leads to a depth of $h = 1.1547\ \mu m$. It should be noted that, unlike blaze gratings, binary gratings are ineffective at a phase shift of 2π. Therefore, the optimum phase shift for binary FGs is at π, which corresponds to a structure depth of $h = 0.577 \mu m$.

3 EXPERIMENTAL SETUP

The fluorine laser is very suitable for processing fused silica and other wide band gap materials, due to the short wavelength of 157 nm (7.9 eV). Moreover, the used mask projection technique allows the fabrication of different optical elements. The laser machine and the appropriate processes are explained detailed in earlier publications (Pfeifer M. et al. 2013, 2014, 2017 and Büttner S. et al. 2019, 2020). Moreover, it is shown that this technology is very flexible. By using different masks and micro structuring methods a whole variety of micro-optical elements can be fabricated. Recapped, there are three options for processing material using the mask projection technique: The movement of a mask within the laser beam and static work piece, the movement of the work piece and a static mask and an all-static setup. Due to the laser source (Lambda Physics LPF220i), the material is removed pulse by pulse. The fabrication process depends on the target microstructure, as well as the mask geometry, which must be adapted too.

The process we developed consists of three steps, the calculation of the grating geometry, the generation of the mask by fluorine laser micro structuring and the generation of the gratings. As mask material we use calcium fluoride (CaF_2) which is transparent for the wavelength of the fluorine laser. The treatment of the polished CaF_2 substrate surface increases the roughness. Due to this, the transmitted radiation is scattered in this area and the energy density is reduced in the corresponding areas within the image of the mask. As result, the mask geometry is transferred into the workpiece. Based on the calculation, the grating patterns were converted into a machine program, which allows the fabrication of the masks itself by fluorine laser micro structuring.

The generated pattern can be scaled up to the required grating size. This should be done in consideration of the feature size and the optical resolution of the imaging system of the laser machine. The up and down scaling is useful for adjusting the optical properties of the grating. To show the possibilities of this technique we calculated and generated five different masks in an CaF_2 substrate (see Figure 2). This technique currently allows the generation of binary structures only, but contrary to using tantalum masks, the layout of the masks in CaF_2 can be individual without compromising of the mechanical stability of the mask.

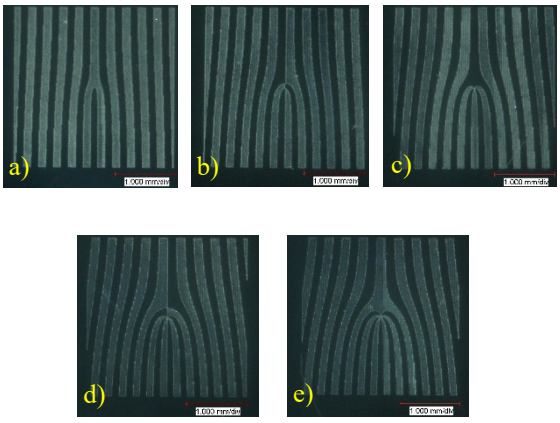

Figure 2: Calcium fluoride masks for the fabrication for fork gratings with a TC of $l = 1,2,3,4,5$ {a), b), c), d), e)}.

4 RESULTS

As mentioned above, we used a static mask design for grating generation. In addition to the CaF_2 grating masks, a 100 x 100 µm² square tantalum mask was used to expose only the corresponding patterned areas of the grating masks to laser radiation. A Slight misalignment of the tantalum and the grating mask leads to structuring errors, as can be seen in Figure 3.

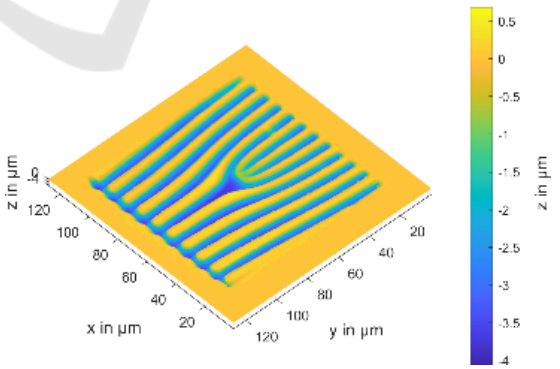

Figure 3: Confocal image of an FG in fused silica Corning 7980.

By using a larger tantalum mask the area surrounding the grating can be lowered such as the grating is exposed. Contrary to expectations, the analysis of the produced structures shows that the

lattice is not binary at all (see Figure 4). The shape of the grating profile section becomes more sinusoidal with increasing number of laser pulses. The grating bars were also influenced by the laser radiation. Therefore, the function of the CaF_2 masks differs from that of the tantalum masks. As can be seen in Figure 5, up to 20 pulses, the depth of the microstructure depends linearly on the number of laser pulses. A further increase of the number of pulses does not increase the depth of the grooves. Therefore, the total depth of the micro structuring is limited.

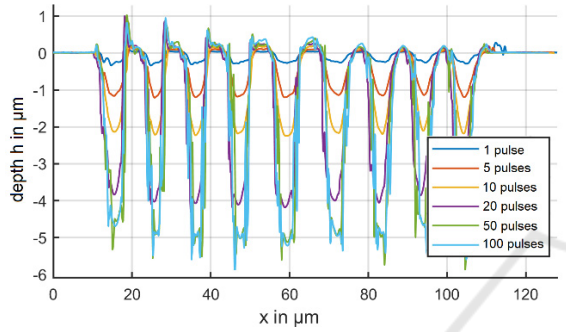

Figure 4: Profile section of the FGs fabricated with different numbers of laser pulses.

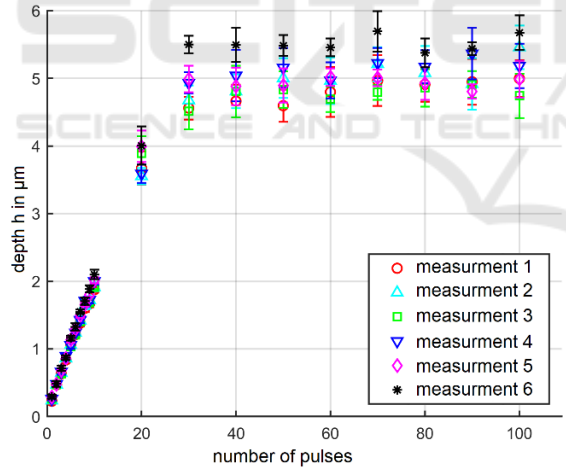

Figure 5: Micro structuring depth depending on the number of laser pulses for different locations within one FG.

For each grating type, this linear dependence was observed up to 20 laser pulses. The maximum depth, on the other hand, depends on the laser pulse fluence and the corresponding ablation depth per pulse. In general, the laser power, the efficiency of the imaging system and the optical parameters of the mask material are the main limiting factors. According to this, a maximum structure depth of 5 µm was reached on average. The period of the grating was set to 20 µm, which results in a feature size of around 10 µm. Therefore, the aspect ratio is limited to a maximum of 2:1. Moreover, the increase of the number of pulses, the grating bars getting higher than the initial surface by the ablation process. This can be explained by the redeposition of material in the areas not having been exposed to radiation. It is currently unclear what the fine structure and optical properties of the redeposited material are, but the influence of the geometry deviations on the function should be significantly stronger. Furthermore, we observed the diffraction image of the gratings, using a microscope and an appropriate laser source for the backside illumination of the optical elements. One diffraction image is shown in Figure 6 a). To see differences in the intensity more clearly, we calculated a colored representation b) of the image.

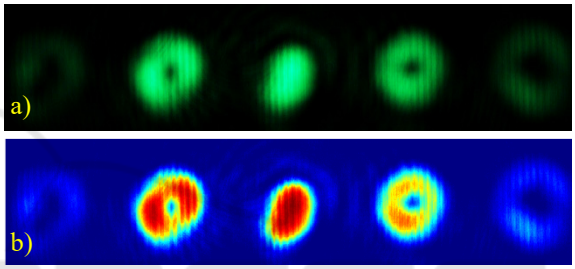

Figure 6: Microscopic diffraction image a) and colored representation b) of the diffraction image of an FG $\{l = 1, h = 0.540\ \mu m\}$.

The FG work as expected. Due to the shape of the grating the intensity is mainly diffracted to the 0^{th} and the $\pm 1^{st}$ diffraction orders. The 0^{th} order does not show any OAM modulation contrary to the higher orders. The modulated diffraction orders show the typical circular shaped intensity distribution of beams with OAM. Moreover, the radius of the distributions increases with the number of the diffraction order due to the increase of the OAM. As can be seen, the radius of 2^{nd} diffraction orders is larger than the one of the 1^{st}. The $\pm 2^{nd}$ diffraction orders are also visible, but the intensity is significantly lower as can be seen. Moreover, the comparison of the $+1^{st}$ and -1^{st} diffraction orders show a slight difference in the intensity distribution. This can be explained by the slightly asymmetric shaped slopes of the grating bars (see Fig 7). Furthermore, the grating grooves are not even, which resulted from a misalignment of the workpiece related to the imaging plane of the optical system. This can be easily corrected but it may also be used to generate defined grating slopes.

Finally, controlling the slope angel opens the opportunity to fabricate blazed gratings using this technique and motivates further investigations.

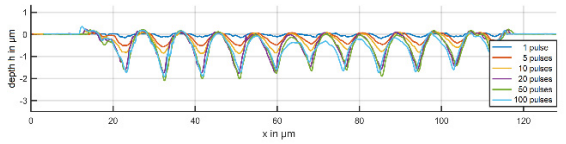

Figure 7: Profile sections of the FGs $\{ l = 1 \}$ fabricated with different numbers of laser pulses.

5 CONCLUSIONS AND OUTLOOK

For the fabrication of FG's, a new method was developed. The process is based on the fluorine laser micro structuring and uses the mask projection technique. The first step is the calculation of the grating pattern and generation of a machine program thereof. Following, the grating layout is transferred into a VUV grade CaF_2 substrate using fluorine laser micro structuring. The VUV grade CaF_2 is transparent for 157 nm radiation, but in the laser treated areas the roughness and therefore the scattering of the radiation is increased. Due to this, the substrate can be used as amplitude mask itself and an individual geometry can be transferred into a fused silica substrate. This was done using different numbers of laser pulses. We could show that the structure depth depends linear on the number of pulses until 20 laser pulses. For more than 20 pulses the depth of the structures does not increase further. Moreover, the structure depth is limited and a maximum aspect ratio of 2:1 can be reached. This represents a limit in feature size range regarding to the target modulation depth. Furthermore, it could be shown that the FG work as expected. The diffraction image shows diffraction orders up to the $\pm 2^{nd}$ order. The asymmetric distribution of intensity is a result from the asymmetric slopes of the grating bars. The reason for this is a slightly misalignment between image plain and surface of the work piece, which easily can be corrected. But potentially this could also be used to generate blazed FG. In general, we could show that the generation of FG's work well and the optical function satisfy our expectations. To improve this, the generation of blazed FG is the next goal of our investigations. An easy and flexible fabrication method for blazed FG's could push forward the OAM multiplexing method due to new possibilities in production of OAM multiplexing hardware.

REFERENCES

Richardson, D. J. (2010). Filling the Light Pipe. In: Science, 330 (6002), pp. 327-328.

Xie, Z.; Gao, S.; Lei, T.; Feng, S.; Zhang, Y.; Li, F.; Zhang, J.; Li, Z.; Yuan, X. (2018). Integrated (de)multiplexer for orbital angular momentum fiber communication. In: Photonics Research, 6(7), pp. 743-749.

Bozinivic, N.; Yue, Y.; Ren, Y.; Tur, M.; Kristensen, P.; Huang, H.; Willner, A.E.; Ramachandran, S. (2013). Terrabit-Scale Orbital Angular Momentum Mode Division Multiplexing in Fibers. In: Science, 340(6140), pp. 1545-1548.

Yao, A.M.; Padgett, M.J. (2011). Orbital Angular Momentum: origins, behaviour and applications. In: Advances in Optics and Photonics, 3, pp. 161-204.

Mair A.; Vaziri, A.; Weihs, G.; Zeilinger, A. (2001). Entanglement of the orbital angular momentum states of photons. In: Nature, 412, pp. 313-316.

Fickler, R.; Lapkiewicz, R.; Plick, W. N.; Krenn, M.; Schaeff, C.; Ramelow, S.; Zeilinger, A. (2012). Quantum Entanglement of High Angular Momenta. Science, 338(6107), 640–643. doi:10.1126/science.1227193

Fickler, Robert; Krenn, Mario; Zeilinger, Anton (2018). Mit Lichtschrauben ans Quantenlimit. Physik in unserer Zeit, 49(1), –. doi:10.1002/piuz.201801494

Allen, L.; Beijersbergen, M.W.; Spreeuw, R.J.C.; Woerdman, J.P. (1992). Orbital angular momentum of light and the transformation of Laguerre-Gaussian laser modes. In: Physical Review A, 45(11), pp. 8185-8189.

Allen, L.; Padget, M. (2011). The Orbital angular momentum of light. In Twisted Photons, WILEY-VCH Verlag GmbH, pp. 1-12, Weinheim.

Marrucci, L.; Manzo, C.; Paparo, D. (2006). Optical Spin-to-Orbital Angular Momentum Conversion in Inhomogeneous Anisotropic Media. Physical Review Letters, 96(16), 163905 doi:10.1103/PhysRevLett.96.163905

Karimi, Ebrahim; Piccirillo, Bruno; Nagali, Eleonora; Marrucci, Lorenzo; Santamato, Enrico (2009). Efficient generation and sorting of orbital angular momentum eigenmodes of light by thermally tuned q-plates. Applied Physics Letters, 94(23), 231124–. doi:10.1063/1.3154549

Pfeifer, M.; Weissmantel, S.; Reisse, G. 2013. Direct laser fabrication of blaze gratings in fused silica. In: Applied Physics A, 112(1), pp. 61-64.

Pfeifer, M.; Jahn, F.; Kratsch, A.; Steiger, B.; Weissmantel, S. 2014. F2-Laser Microfabrication of Diffractive Optical Elements. In: Proceedings of 2nd International Conference on Photonics, Optics and Laser Technology, pp. 91-96.

Pfeifer, M.; Büttner, S.; Zhang, R.; Serbay, M.; Weißmantel, S. (2017). F2-Lasermikrostrukturierung von Mikro-Fresnel-Linsen, In: Scientific Reports, 10. Mittweidaer Lasertagung, (2), pp. 127-130.

Büttner, S.; Pfeifer, M.; Weissmantel, S. (2019). Manufacturing of Cylindrical Micro Lenses and Micro

Lens Arrays in Fused Silica and Borosilicate Glass using F2-Laser Microstructuring. In: Proceedings of 7th International Conference on Photonics, Optics and Laser Technology, pp. 66-72.

Büttner, S.; Pfeifer, M.; Weissmantel, S. (2020). Fabrication of Micro Spiral Phase Plates in Fused Silica using F2-Laser Microstructuring. In: Proceedings of 8th International Conference on Photonics, Optics and Laser Technology, pp. 114-121.

Galvez, E.: Computer Program FORKED DIFFRACTION PATTERN, Version 1.0 (2016), WWW Document: (http://departments.colgate.edu/physics/gpl.htm).